

REORDER: Securing Dynamic-Priority Real-Time Systems Using Schedule Obfuscation

Chien-Ying Chen*, Monowar Hasan*, AmirEmad Ghassami, Sibin Mohan and Negar Kiyavash
University of Illinois at Urbana-Champaign, Urbana, USA
{cchen140, mhasan11, ghassam2, sabin, kiyavash}@illinois.edu

Abstract—Modern real-time systems (RTS) are increasingly the focus of security threats. The design of such systems often aids attackers since RTS are engineered to be predictable. This predictability can be used to mount side-channel attacks, destabilize the system (by denying access to critical resources at important times), *etc.* In this paper, we propose methods to *obfuscate* the predictable (scheduling) behavior of RTS that use dynamic-priority real-time scheduling algorithms (*e.g.*, EDF). We developed the REORDER protocol for this purpose. Such obfuscation will make it difficult for attackers to target RTS. We also developed a metric (called “schedule entropy”) to measure the amount of obfuscation. We integrated our REORDER protocol into the Linux real-time EDF scheduler and evaluated our scheme using both – a realistic embedded platform based on Raspberry Pi and also synthetic workloads.

I. INTRODUCTION

Security is increasingly becoming an important domain for real-time systems (RTS). Malicious entities can cause significant damage to critical systems with real-time properties unless such systems have good security mechanisms embedded within them at design time. Until recently, security was an afterthought in RTS but that is changing with the advent of high-profile attacks (*e.g.*, denial-of-service attacks using Internet-of-Things devices [1], Stuxnet [2], BlackEnergy [3], *etc.*). The rise in the use of common-off-the-shelf (COTS) components as well as emerging technologies (*e.g.*, Internet-of-Things) only exacerbates these problems.

Systems with real-time properties are predictable by design. As such, this property can be used to improve the security of such systems [4]–[6]. On the other hand, this very determinism can become a vulnerability in the hands of smart adversaries. Once attackers are able to reconstruct the timing behavior of RTS, they can predict, in a precise manner, the schedule of all tasks in the system for the foreseeable future. Most hard RTS are designed to be periodic/sporadic in nature and the tasks running on such systems are characterized and constrained by their periods and deadlines. Due to the strict periodicity of the real-time tasks, the schedule repeats every hyperperiod. Hence, it becomes easier to carry out adversarial actions such as side-channel attacks [7], [8], DoS (making critical resources unavailable at important times) or even the recently developed timing-inference attacks [7]. Naive techniques to obfuscate the timing information or schedules [9], while improving security, could result in missed deadlines – leading to catastrophic events such as system failure, damage to the environment or even loss of human life. Hence, there is a need to ensure that we *reduce the determinism that is visible to external entities while still meeting real-time guarantees*.

While there exists some recent work on defensive techniques for real-time systems (*e.g.*, [4], [5], [10]–[15]), only

a few focus on scheduling algorithms [9], [16]. One reason is the belief that the scheduler has limited resources; thus it is often overlooked while considering the development of security measures. Nevertheless, the scheduler is still one of the most effective places to defend against the aforementioned attacks. As a result, we believe that a technique that works at the scheduler level will be effective in preventing such attacks.

One way to prevent such attacks from succeeding is by *obfuscating the schedule* – *i.e.*, introduce randomness into the execution patterns so that the schedule varies between hyperperiods. This way, even if attackers are able to reconstruct all (or part of) a hyperperiod, they will not be able to predict future execution patterns. Existing work [9], [16] either focuses on static priority algorithms or measure the effects of such obfuscation inadequately.

In this paper, we propose a schedule randomization framework, that we refer to as REORDER (REal-time ObfuscateR for Dynamic scheduler). The REORDER framework extends ideas from prior work [9]. While our previous work is based on the fixed-priority scheduling algorithms (*e.g.*, rate monotonic (RM) [17]), in this paper we focus on the earliest deadline first (EDF) scheduling policy. EDF is a dynamic scheduler that offers full CPU utilization capabilities and is used in many real-time operating systems (such as Erika Enterprise [18], RTEMS [19], real-time Linux [20], *etc.*). We implemented REORDER in a real-time Linux kernel and also evaluated it on an embedded platform. We show that if a real-time system meets its timing guarantees when scheduled by vanilla EDF, then the REORDER framework will also ensure the same guarantees. In addition, we also developed a metric (named “schedule entropy”) that measures the amount of obfuscation for each schedule when REORDER is used. This can be used to capture the amount of randomness that is introduced into the system and can also be used to compare different schedules (in their effectiveness to obfuscate the schedules).

In this paper we make the following contributions:

- a randomization algorithm that shuffles EDF schedules (Section III).
- a new metric for calculating the entropy in the system (Section IV).
- an implementation of the REORDER protocol in the Linux kernel (Section V).

We next discuss the system and adversary models.

II. SYSTEM AND ADVERSARY MODEL

A. Real-time Task and Scheduling Models

Let us consider the problem of scheduling a set of n periodic tasks $\Gamma = \{\tau_1, \tau_2, \dots, \tau_n\}$ on a single processor, using the EDF scheduling policy. In this work we focus on the widely used periodic task model [21] in which each task $\tau_i \in \Gamma$ is

*These authors contributed equally to this work.

characterized by the tuple (C_i, T_i, D_i) where C_i is the worst-case execution time (WCET), T_i is the period and D_i is the relative deadline. We denote d_i as the absolute deadline of τ_i . We do not consider any precedence or synchronization constraints among tasks and $C_i, T_i, D_i \in \mathbb{N}^+$, $\forall \tau_i \in \Gamma$. For the simplicity of notation, we use the same symbol τ_i to denote its jobs and use the term *task* and *job* interchangeably.

We assume that the tasks have constrained-deadlines, i.e., $D_i \leq T_i$, $\forall \tau_i$ and the taskset is *schedulable* by the EDF scheduling policy. Since the taskset is schedulable, the following (necessary and sufficient) condition will hold [22]: $\sum_{\tau_i \in \Gamma} \text{DBF}(\tau_i, t) \leq t$, $\forall t \geq 0$ where the *demand bound function* $\text{DBF}(\tau_i, t)$ computes the cumulative maximum execution requirements of all jobs of τ_i (each of whose release time and deadline are within the interval t) and defined as follows: $\text{DBF}(\tau_i, t) \stackrel{\text{def}}{=} \max \left(0, \left(\left\lfloor \frac{t-D_i}{T_i} \right\rfloor + 1 \right) C_i \right)$.

Under the periodic task model, the schedule produced by any preemptive scheduling policy over a periodic taskset is cyclic, that is, the system will repeat the task arrival pattern after an interval that coincides with the taskset's *hyperperiod* [23], denoted by L . Furthermore, we consider a discrete time model (e.g., integral time units [24]) where system and task parameters are multiples of a time unit¹.

B. Adversary Model

We assume that the attackers have access to the timing parameters of the tasksets and also have knowledge of which scheduling policy is being used. The adversary's objective is to get detailed information about the execution patterns of the real-time tasks and cause greater damage to the system by exploiting such precise schedule information [7]. The attacker may exploit some side-channels to observe (and reconstruct) the system schedule. A smart attacker possessing sufficient system information can carry out some collaborative attacks under the right conditions to move the system to an unsafe state. For example, in the now famous Stuxnet [2] attack, the malware remains in the system for *months* to collect sensitive information before it proceeds with the main attack. It is possible for a denial-of-service attack to target only a specific service handled by a critical task when the precise schedule information is obtainable. A side-channel attack [25], [26] is also another typical class of attacks that can benefit from such schedule reconstruction attacks. For example, it was shown that the precise schedule information can be exploited to assist in determining the *prime* and *probe* [27] instants in a cache side-channel attack to increase the chance of success [7].

We further assume that the scheduler is not compromised and the attacker does not have access to the scheduler. Without this assumption, the attacker can undermine the scheduler or directly obtain the schedule information. This is a reasonable assumption since the scheduler operates with administrative privileges and attacks at the application level are easier. Security mechanisms that prevent unauthorized access to the root privileges can improve the security of the scheduler.

III. SCHEDULE RANDOMIZATION PROTOCOL

In this section we describe the REORDER protocol whose objective is to reduce the inferability of the schedule for real-time tasksets. The focus of our design is such that, even

if an observer is able to capture the exact schedule for a (limited) period of time (for instance, for a few hyperperiods), REORDER will schedule tasks in a way that succeeding hyperperiod will show *different orders (and timing) of execution* for the tasks. The main idea is that at each scheduling point, we *pick a random task from the ready queue* and schedule it for execution. However such random selection may lead to priority inversions [28] and any arbitrary selection may result in *missed deadlines* – hence, putting at risk the safety of the system. REORDER solves this problem by allowing *bounded priority inversions*. It restricts how the schedule may use priority inversions without violating real-time constraints (e.g., deadline) of the tasks. To ensure this, REORDER *calculates an “acceptable” priority inversion budget*. If the budget is exhausted during execution, then we stop allowing lower priority tasks to execute ahead of the higher priority task with the empty budget. The following sections present the details of the REORDER protocol.

A. Randomization with Priority Inversion

A key step for randomization is to calculate the maximum amount of time that lower priority jobs, $lp(\tau_i), \tau_i \in \Gamma$, can execute before τ_i . This is much harder in EDF compared to the fixed-priority system (that prior work [9] was focused on) due to the dynamic nature of EDF (i.e., the task priority varies in run-time). Therefore we define the *worst-case inversion budget* (WCIB) V_i that represents the maximum amount of time for which a job of some task τ_i with relative deadline d_i may be blocked by a job of some task $\tau_j \in \Gamma, j \neq i$ with $d_j > d_i$. In the following we illustrate how we calculate WCIB for each task by utilizing the response time analysis [29], [30] for EDF.

1) *Bounding Priority Inversions*: The worst-case response time (WCRT) of τ_i is the maximum time between the arrival of a job of τ_i and its completion. Under EDF, the response time calculation involves computing the busy-period² of a task's instance with deadline less than or equal to that instance [30]. To calculate the WCIB of a task, we measure the worst-case interference from its higher priority jobs. Note that with arbitrary priority inversions, any job could be delayed because of chain reactions, i.e., some low priority jobs in $lp(\tau_i)$, delay the higher priority jobs (e.g., $\tau_j, \forall d_j < d_i$), that in turn delay τ_i – hence τ_i may need more than its WCRT calculated by the response time analysis. This phenomenon is known as back-to-back hit [32] and can be addressed by considering an extra instance of higher priority jobs. Therefore, without any assumptions on the execution patterns of $lp(\tau_i)$, for a given release time $t = a$ we can calculate the upper bound of interference experienced by τ_i as follows [29], [30], [32]:

$$I_i(a) = \sum_{j \neq i, D_j \leq a+D_i} \min \left\{ \left\lfloor \frac{D_i}{T_j} \right\rfloor + 1, 1 + \left\lfloor \frac{a + D_i - D_j}{T_j} \right\rfloor + 1 \right\} C_j. \quad (1)$$

Note that the extra execution times (e.g., +1 in Eq. (1)) are added in the interference calculation to prevent the effects of back-to-back hit from higher priority jobs. For a given release time a , the response time of τ_i relative to a is given by [29], [30]: $R_i(a) = \max \{C_i, W_i(a) - a\}$ where $W_i(a) = \left(\left\lfloor \frac{a}{T_i} \right\rfloor + 1 \right) C_i + I_i(a)$ and $I_i(a)$ is calculated by Eq.

²A busy-period [31] of τ_i is the interval $[t_0, t]$ within which jobs with priority higher or equal than τ_i are processed throughout $[t_0, t]$ but no jobs with priority higher or equal than τ_i are processed in $t_0 - \epsilon, t_0$ or $(t, t + \epsilon)$ for a sufficiently small ϵ .

¹We denote an interval starting from time point a and ending at time point b that has a length of $b - a$ by $[a, b)$ or $[a, b - 1]$.

(1). Finally we can compute the upper bound of WCRT of τ_i as follows:

$$R_i = \max \{R_i(a)\}, \quad 0 \leq a < \widehat{R} - C_i \quad (2)$$

where $\widehat{R} = r^{(k+1)} = r^{(k)}$ for some k and $r^{(\cdot)}$ is the upper bound of any busy-period length and can be calculated by the following recurrence relation:

$$r^{(0)} = \sum_{\tau_i \in \Gamma} C_i, \quad r^{(k+1)} = \sum_{\tau_i \in \Gamma} \left\lceil \frac{r^{(k)}}{T_i} \right\rceil C_i. \quad (3)$$

The above sequence $r^{(k)}$ converges to \widehat{R} in a finite number of steps if we assume that the taskset is schedulable (i.e., $\sum_{\tau_i \in \Gamma} \frac{C_i}{T_i} \leq 1$) [30]. Based on the above calculations, we can derive the WCIB of τ_i as follows:

$$V_i = D_i - R_i. \quad (4)$$

The WCIB V_i represents the maximum amount of time for which all lower priority jobs $lp(\tau_i)$ (e.g., $d_j > d_i$) are allowed to execute while an instance of τ_i is still unfinished without missing its deadline even in the worst-case scenario. The REORDER protocol guarantees that the real-time constraints are satisfied by bounding priority inversions using $V_i, \forall \tau_i \in \Gamma$. Note that WCIB can be negative for some τ_i . At each scheduling point t , our idea is to execute some low priority job τ_j with $V_j > 0$ up to $\min(\widehat{C}_j^t, V_j)$ additional time-units before it leaves the processor for highest priority job where \widehat{C}_j^t represents the remaining execution time of τ_j at t .

We enforce WCIB at run-time by maintaining a per-job counter, *remaining inversion budget* (RIB) $v_i, 0 \leq v_i \leq V_i$. The counter RIB is initialized to V_i upon each activation of jobs of τ_i and decremented for each time unit when τ_i is blocked by any lower priority job. When v_i reaches zero no job with absolute deadline greater than d_i is allowed to run until τ_i completes.

Note that the worst-case interference that τ_i can experience is bounded by $\max\{I_i(a)\}, 0 \leq a < \widehat{R} - C_i$. Besides, for a given non-negative WCIB, jobs of τ_i can be delayed for up to V_i by priority inversions. The WCRT of τ_i is bounded by $R_i + V_i = R_i + D_i - R_i = D_i$. Hence, τ_i is schedulable with the REORDER protocol and we can assert the following:

Proposition 1. *If Γ is schedulable under EDF, WCIB is non-negative for some τ_i and low priority jobs of τ_i do not delay τ_i more than V_i then REORDER will not violate the real-time constraints of τ_i .*

2) *Selection of Candidate Jobs for Randomization:* As we mentioned earlier, when the run-time counter RIB, v_i , reaches zero no jobs with deadline greater than d_i can run while τ_i has an outstanding job. However, lower priority jobs could cause τ_i to miss its deadline by inducing the worst-case interference from the higher priority jobs, i.e., $\forall d_j < d_i$, due to the chain reaction. Therefore, to preserve the schedulability of such jobs we must prevent it from experiencing such additional delays. We achieve this by defining the following inversion policy:

► **Randomization Priority Inversion Policy (RPIP):** *If RIB $v_i < 0$ for some $\tau_i \in \Gamma$, no job τ_j with $d_j > d_i$ is allowed to run while any of high priority job τ_k with $d_k < d_i$ has an unfinished job.*

In order to enforce RPIP at run-time, at each scheduling decision point, we now define the variable minimum inversion

deadline m_i^t for jobs of τ_i as follows:

$$m_i^t = \min\{d_j | \tau_j \in \mathcal{R}_Q^t, d_j > d_i \wedge (v_j < 0 \text{ or } V_j < 0)\}. \quad (5)$$

where \mathcal{R}_Q^t is the ready queue at scheduling point t . When there is no such task as τ_j , m_i^t is set to an arbitrarily large (e.g., infinite) deadline. The variable m_i^t allows us to determine which jobs to *exclude* from priority inversions. That is, no job that has a higher deadline than m_i^t can be scheduled as long as τ_i has an unfinished job. Otherwise, the job with relative deadline m_i^t (not the job τ_i) could miss its deadline. As an example, let us consider the following taskset:

Example 1. *The taskset $\Gamma_{ex1} = \{\tau_1, \tau_2, \tau_3, \tau_4\}$ contains the following parameters:*

Task	C_i	$T_i = D_i$	V_i
τ_1	4	10	1
τ_2	1	20	-2
τ_3	1	5	-2
τ_4	2	12	-1

At $t = 0$, $d_1 = 10$, $d_2 = 20$, $d_3 = 5$, $d_4 = 12$. For notational convenience, let us denote m_i^0 as m_i . Hence $m_1 = 12$, $m_2 = \infty$, $m_3 = 12$ and $m_4 = 20$. Therefore at $t = 0$ the job τ_2 and τ_4 are not allowed to participate in priority inversion (since $d_2, d_4 > m_i, i \in \{1, 3\}$ and τ_1, τ_3 are not completed).

It can be shown that at any scheduling point t we can enforce RPIP by only examining the inversion deadline of highest priority (e.g., shortest deadline) job, m_{HP}^t [9]. Hence, at each scheduling decision, REORDER excludes all ready jobs from the selection that have higher deadline than m_{HP}^t .

B. Overview of The Randomization Protocol

We now present the overview of the REORDER protocol. The protocol selects a new job using the following sequence of steps (refer to Algorithm 1 in the Appendix for a formal description) whenever at every scheduling decision point.

- **Step 1 (Candidate Selection):** At each scheduling point t , the REORDER protocol searches for possible candidate jobs (that can be used for priority inversion) in the ready queue. Let us denote \mathcal{R}_Q^t as the set of ready jobs, $\tau_{HP} \in \mathcal{R}_Q^t$ is the highest priority (i.e., shortest deadline) job in the ready queue and \mathcal{C}_L^t represents the set of candidate jobs at some scheduling point t .
 - We first check the counter RIB of the highest priority job $\tau_{HP} \in \mathcal{R}_Q^t$. If the RIB is zero, then τ_{HP} is added to the candidate and REORDER moves to Step 2 since priority inversion is not possible due to its inversion budget being non-positive.
 - Otherwise (i.e., when $v_{HP} > 0$), we iterate through the ready queue and add the job $\tau_i \in \mathcal{R}_Q^t$ to the candidate list \mathcal{C}_L^t if its deadline is smaller than or equal to m_{HP}^t , i.e., the minimum inversion deadline of the highest-priority job at scheduling point t .
- **Step 2 (Random Schedule):** This step (randomly) selects a job from the ready queue for scheduling. The job selected at this step will run until the next scheduling decision point t' . We randomly pick a job τ_R from \mathcal{C}_L^t and set the next scheduling decision point as follows:
 - If τ_R is the highest priority job in the ready queue, the next decision point t' will be either when the job finishes or a new job of another task arrives.

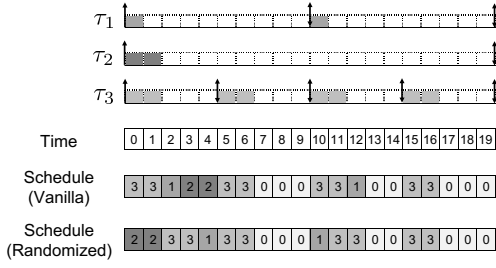


Fig. 1. An instance of schedule randomization protocol. The length of the taskset hyperperiod is $L = 20$ and 0 represents idle time (e.g., when no other tasks are active). The upward and downward arrows represent job activations and deadlines, respectively.

- Otherwise, the next decision³ will be made at when τ_R completes or the inversion budget expires, that is,

$$t' = t + \min(\widehat{C}_R^t, \widehat{v}), \quad (6)$$

unless a new job arrives before time t' where

$$\widehat{v} = \min(v_j | \tau_j \in \mathcal{R}_Q^t \wedge d_j < d_R) \quad (7)$$

and \widehat{C}_R^t represents the remaining execution time of τ_R . Note that the variable \widehat{v} is always positive since every job with a higher priority than the selected job has some remaining inversion budget. Otherwise, τ_R would not have been added to the candidate list in Step 1.

We now illustrate the ideas of our randomization protocol using a simple example.

Example 2. Let us consider the taskset $\Gamma_{ex2} = \{\tau_1, \tau_2, \tau_3\}$ with following parameters:

Task	C_i	$T_i = D_i$	V_i
τ_1	1	10	3
τ_2	2	20	5
τ_3	2	5	3

The taskset is schedulable by EDF (e.g., $\sum_{\tau_i \in \Gamma_{ex2}} \frac{C_i}{T_i} \leq 1$). The schedule of the vanilla EDF and an instance of randomization protocol is illustrated in Fig. 1. At time $t = 0$, all three jobs are in ready queue and have positive inversion budget. Notice that τ_3 is the highest priority job, $m_{HP} = \infty$ and all three jobs are in the candidate list. Let the scheduler randomly picks τ_2 . From Eq. (6), the next scheduling decision will be taken at $t = 0 + \min(2, 3) = 2$. At $t = 1$, $v_1 = v_3 = 1$, $m_{HP} = m_3 = \infty$ and both τ_1 and τ_3 are in candidate list. Let τ_3 be randomly scheduled (that is also the highest priority job). The next scheduling decision will be at $t = 2 + 2 = 4$. At $t = 4$, only τ_1 is active and scheduled (next scheduling decision will be at $t = 5$). τ_3 is the only active job at time $t = 5$ and hence scheduled. At $t = 10$, both τ_1 and τ_3 are active, $m_3 = m_{HP} = \infty$ and hence both are in candidate list. τ_1 is randomly scheduled and the next scheduling point will be at $t = 10 + 1 = 11$. At $t = 11$, only τ_3 is active and scheduled. Likewise, τ_3 is the only active job at $t = 15$ and scheduled.

In Fig. 2(a) we illustrate the EDF schedule of the taskset from Example 2 for 15 hyperperiods where each row in the figure represents one hyperperiod. The numbers $i \in \{1, 2, 3\}$

³In Section III-D, we present another approach to trigger the scheduling decisions.

HP1	3	3	1	2	2	3	3	0	0	0	3	3	1	0	0	3	3	0	0
HP2	3	3	1	2	2	3	3	0	0	0	3	3	1	0	0	3	3	0	0
HP3	3	3	1	2	2	3	3	0	0	0	3	3	1	0	0	3	3	0	0
HP4	3	3	1	2	2	3	3	0	0	0	3	3	1	0	0	3	3	0	0
HP5	3	3	1	2	2	3	3	0	0	0	3	3	1	0	0	3	3	0	0
HP6	3	3	1	2	2	3	3	0	0	0	3	3	1	0	0	3	3	0	0
HP7	3	3	1	2	2	3	3	0	0	0	3	3	1	0	0	3	3	0	0
HP8	3	3	1	2	2	3	3	0	0	0	3	3	1	0	0	3	3	0	0
HP9	3	3	1	2	2	3	3	0	0	0	3	3	1	0	0	3	3	0	0
HP10	3	3	1	2	2	3	3	0	0	0	3	3	1	0	0	3	3	0	0
HP11	3	3	1	2	2	3	3	0	0	0	3	3	1	0	0	3	3	0	0
HP12	3	3	1	2	2	3	3	0	0	0	3	3	1	0	0	3	3	0	0
HP13	3	3	1	2	2	3	3	0	0	0	3	3	1	0	0	3	3	0	0
HP14	3	3	1	2	2	3	3	0	0	0	3	3	1	0	0	3	3	0	0
HP15	3	3	1	2	2	3	3	0	0	0	3	3	1	0	0	3	3	0	0

(a) Vanilla EDF (no randomization)

HP1	1	3	3	2	2	3	3	0	0	0	3	3	1	0	0	3	3	0	0
HP2	2	2	3	3	1	3	3	0	0	0	3	3	1	0	0	3	3	0	0
HP3	1	3	3	2	2	3	3	0	0	0	3	3	1	0	0	3	3	0	0
HP4	2	2	3	3	1	3	3	0	0	0	1	3	3	0	0	3	3	0	0
HP5	3	3	1	2	2	3	3	0	0	0	1	3	3	0	0	3	3	0	0
HP6	3	3	2	2	1	3	3	0	0	0	3	3	1	0	0	3	3	0	0
HP7	2	2	3	3	1	3	3	0	0	0	3	3	1	0	0	3	3	0	0
HP8	1	3	3	2	2	3	3	0	0	0	3	3	1	0	0	3	3	0	0
HP9	3	3	2	2	1	3	3	0	0	0	3	3	1	0	0	3	3	0	0
HP10	1	3	3	2	2	3	3	0	0	0	1	3	3	0	0	3	3	0	0
HP11	1	3	3	2	2	3	3	0	0	0	3	3	1	0	0	3	3	0	0
HP12	1	3	3	2	2	3	3	0	0	0	3	3	1	0	0	3	3	0	0
HP13	2	2	3	3	1	3	3	0	0	0	3	3	1	0	0	3	3	0	0
HP14	3	3	2	2	1	3	3	0	0	0	3	3	1	0	0	3	3	0	0
HP15	3	3	2	2	1	3	3	0	0	0	1	3	3	0	0	3	3	0	0

(b) Randomization (task only)

HP1	0	0	0	3	3	1	2	2	3	3	1	3	3	0	0	3	3	0	0
HP2	2	2	3	3	1	3	3	0	0	0	3	3	1	0	0	3	3	0	0
HP3	0	0	0	3	3	1	3	3	2	2	1	3	3	0	0	3	3	0	0
HP4	1	3	3	2	2	3	3	0	0	0	1	3	3	0	0	3	3	0	0
HP5	0	0	0	3	3	1	2	2	3	3	3	3	1	0	0	3	3	0	0
HP6	2	2	3	3	1	0	0	0	3	3	0	3	3	1	0	0	3	3	0
HP7	1	3	3	2	2	3	3	0	0	0	3	3	1	0	0	3	3	0	0
HP8	1	3	3	2	2	3	3	0	0	0	3	3	1	0	0	0	3	3	3
HP9	1	3	3	2	2	0	0	0	3	3	1	3	3	0	0	3	3	0	0
HP10	2	2	3	3	1	0	0	0	3	3	3	3	1	0	0	3	3	0	0
HP11	3	3	1	2	2	3	3	0	0	0	3	3	0	1	0	0	0	3	3
HP12	3	3	1	2	2	3	3	0	0	0	0	0	3	3	1	3	3	0	0
HP13	1	3	3	2	2	3	3	0	0	0	3	3	0	1	0	3	3	0	0
HP14	1	3	3	2	2	3	3	0	0	0	1	3	3	0	0	3	3	0	0
HP15	3	3	1	2	2	3	3	0	0	0	3	3	0	1	0	0	0	3	3

(c) Randomization with idle time

HP1	0	3	3	1	2	2	3	3	0	0	2	1	3	3	0	0	0	3	3	0	0
HP2	3	3	0	1	2	2	3	3	2	0	0	1	3	3	0	0	0	3	3	0	0
HP3	2	3	3	1	0	3	3	2	0	0	1	3	3	0	0	0	3	3	0	0	
HP4	0	3	3	1	2	2	3	3	0	0	1	3	3	0	0	0	3	3	0	0	
HP5	3	3	2	1	2	2	3	3	0	0	0	3	3	1	0	0	0	3	3	0	0
HP6	1	3	3	0	0	3	3	2	2	0	3	3	0	1	0	0	3	3	0	0	
HP7	1	3	3	2	2	0	3	3	0	0	0	3	3	1	0	0	0	3	3	0	0
HP8	0	3	3	1	0	3	3	2	2	0	3	3	0	1	0	0	0	3	3	0	0
HP9	0	3	3	1	2	2	3	3	0	0	0	3	3	1	0	0	0	3	3	0	0
HP10	0	3	3	1	2	0	3	3	2	0	1	3	3	0	0	0	0	3	3	0	0
HP11	3	3	0	1	0	0	3	3	2	2	1	3	3	0	0	0	0	3	3	0	0
HP12	3	3	0	1	2	0	3	3	2	0	0	3	3	1	0	0	0	3	3	0	0
HP13	2	3	3	1	0	2	3	3	0	0	0	3	3	1	0	0	0	3	3	0	0
HP14	0	3	3	1	0	0	3	3	2	2	3	3	1	0	0	0	0	3	3	0	0
HP15	1	3	3	2	2	0	3	3	0	0	1	3	3	0	0	0	0	3	3	0	0

(d) Randomization with idle time and fined-grained switching

Fig. 2. Illustration of vanilla EDF and different randomization schemes. The figure depicts the schedule of 15 hyperperiods for the taskset in Example 2.

in each slot represent the tasks $\tau_i \in \Gamma_{ex2}$ and 0 represents idle time. Due to the nature of EDF, the schedule is predictable since the same pattern repeats after each hyperperiod ($L = 20$ in this example). The schedule generated by the randomization protocol is depicted in Fig. 2(b). As seen from the figure our randomization protocol brings variation between the hyperperiods compared to the vanilla EDF – albeit some of the randomized tasks in different hyperperiods appear in similar places. The schedule is therefore somewhat predictable since the idle times (i.e., slack) appear in same slots. We address this problem by *scrambling the idle slots* along with the real-time tasks in the next section.

C. Idle Time Scheduling

One of the limitations of randomizing only the tasks is that the task execution is squeezed between the idle time slots

– the latter remain predictable. The work-conserving nature of EDF causes separations between task executions and idle times. Hence some tasks appear at similar places over multiple hyperperiods. One way to address this problem and improve schedule randomness is to *idle the processor*, intentionally, at random times [9]. We achieve this by considering idle times as instances of an additional task, referred to as the *idle task*, τ_I . Then, the randomization protocol can be applied over the *augmented taskset* $\Gamma' = \Gamma \cup \{\tau_I\}$. The schedule generated for $\Gamma'_{ex} = \Gamma_{ex} \cup \{\tau_I\}$ is illustrated in Fig. 2(c) where 0 represents τ_I . As the figure shows the tasks are spread over wider ranges compared to Fig. 2(b).

It can be noted that τ_I has infinite period, deadline and execution time, and hence always executes with the *lowest* priority. Hence τ_I can force all other tasks $\tau_i \in \Gamma$ to maximally consume their inversion budgets. During randomization the idle task will convert a work-conserving schedule to a non-work-conserving one, but it will not cause any starvation for other tasks. This is because Step 2 of the REORDER protocol (see Section III-B) selects candidate tasks in a way that real-time constraints for *all* tasks in the system will always be respected. Randomizing the idle task effectively makes tasks appear across wider ranges and thus reduces predictability. As a result, the schedule can be less susceptible to attacks that depend on the predictability of RTS.

D. Fine-Grained Switching

In prior work [9] we proposed to decrease the inferability of the fixed-priority scheduler by randomly *yielding* a job, early, during execution. As a result the schedule will be fragmented at different time-points and thus will bring more variations across hyperperiods. The proposed REORDER protocol can also be modified to incorporate such a feature. Recall that the scheduling decisions in our scheme are made either when: (i) a new job arrives, (ii) a job completes, or (iii) the inversion budget expires (refer to Step 2 in Section III-B). Therefore we can achieve the fine-grained switching by modifying the next scheduling decision point t' in Eq. (6) as follows:

$$t' = t + \text{rand}(1, \min(\widehat{C}_R^t, \widehat{v})) \quad (8)$$

where the function $\text{rand}(a, b)$ outputs a random number between $[a, b]$. In Fig. 2(d) we illustrate the schedule of Γ'_{ex} using the fine-grained randomization scheme. While some tasks are completed earlier (for this specific taskset and randomization instance) and leaving the idle tasks for later slots, it does not attribute that this scheme is inferior than the previous one.

IV. SCHEDULE ENTROPY: A MEASURE OF RANDOMNESS

While the mechanisms presented in Algorithm 1 obfuscates the inherent determinism in conventional dynamic-priority schedules, we still need to *quantify the randomness* that has been introduced into the schedule. This can be addressed by analyzing the *schedule entropy* [9] that measures the randomness (or unpredictability) in the real-time schedule. In the following, we first describe the limitations of existing entropy calculation techniques [9] and then introduce a better approach to measure the schedule entropy, followed by an evaluation of the entropy of the various schemes using synthetic workloads.

A. Limitations of Existing Entropy Calculation Approach

In order to evaluate the performance of a randomized scheduler, we need to have a measure of the randomness of the output of the scheduler. For a taskset with hyperperiod of length L , define the L dimensional random vector $\mathcal{S}^k = [S_1^k, \dots, S_L^k]$ representing the schedule of hyperperiod k , where the random variable $S_t^k \in \{\tau_0, \dots, \tau_n\}$ denotes the task (including the idle task) scheduled at the t -th slot of hyperperiod k . Note that the random vectors \mathcal{S}^k for different values of k are independent and identically distributed (i.i.d.) random variables. Therefore the average randomness of the whole output is equal to the randomness in a single hyperperiod.

In the past [9], we have defined the entropy of the schedule \mathcal{S}^k using Shannon entropy [33, Ch. 2] as a measure of the randomness, *i.e.*:

$$H(\mathcal{S}^k) = - \sum_{s_1^k \in \{\tau_0, \dots, \tau_n\}} \dots \sum_{s_L^k \in \{\tau_0, \dots, \tau_n\}} \mathbb{P}(\mathcal{S}^k = [s_1, \dots, s_L]) \times \log_2 \mathbb{P}(\mathcal{S}^k = [s_1, \dots, s_L]) \quad (9)$$

with the assumption that $0 \times \log_2 0 = 0$.

There are two major issues in calculating the schedule entropy using the above method. *First*, in order to obtain $H(\mathcal{S}^k)$, we need to calculate the distribution $\mathbb{P}(\mathcal{S}^k)$ – calculating this distribution has exponential complexity and is not computationally tractable in practice. Also, estimating this distribution requires a very high number of samples. To address this problem, we proposed [9] to use the sum of the entropy of random variables S_t^k , $t \in \{1, \dots, L\}$ as the measure of randomness (referred to as upper-approximated schedule entropy):

$$\widetilde{H}(\mathcal{S}^k) = \sum_{t=1}^L H(S_t^k), \quad (10)$$

where $H(S_t^k) = - \sum_{s_t^k \in \{\tau_0, \dots, \tau_n\}} \mathbb{P}(S_t^k = s_t^k) \log_2 \mathbb{P}(S_t^k = s_t^k)$. The main limitations of upper approximated schedule entropy $\widetilde{H}(\mathcal{S}^k)$ is that it completely ignores the regularities that exist in \mathcal{S}^k due to the dependencies among random variables. For instance, suppose a taskset contains two tasks: $\Gamma = \{\tau_1, \tau_2\}$ and a schedule for first 5 slots in 2 individual hyperperiods is as follows: $\mathcal{S}_1 \in \{(\tau_1, \tau_2, \tau_1, \tau_2, \tau_1), (\tau_2, \tau_1, \tau_2, \tau_1, \tau_2)\}$, assuming each vector with equal probability. Let us consider another schedule \mathcal{S}_2 that has all possible 2^5 vectors of τ_1 and τ_2 of length 5 with equal probability. Then $\widetilde{H}(\mathcal{S}_1) = \widetilde{H}(\mathcal{S}_2)$ even though the randomness of \mathcal{S}_2 is much higher (*i.e.*, $H(\mathcal{S}_1) = 1$ while $H(\mathcal{S}_2) = 5$). Therefore, $\widetilde{H}(\mathcal{S}^k)$ cannot capture the randomness correctly.

Second, consider an instance where many of the schedules produced in different hyperperiods have very similar patterns in the first few slots and different patterns in the latter slots (or vice versa). In such cases $H(\mathcal{S}^k)$ cannot capture the similarities and considers the observed hyperperiods as distinct ones – this leads us to search for dissimilarities in *intervals* smaller than the whole length of the hyperperiod. In what follows we propose an entropy measure to capture the randomness of a schedule using the concept of *limited size intervals* that resolves both the aforementioned issues and provides a better way to quantitatively compute randomness.

B. Entropy of a REORDER Schedule

The proposed concept is based on a statistical model – *approximate entropy (ApEn)* [34] that is used to evaluate the amount of regularity in time series data. Let us consider $K > 1$ hyperperiods for a taskset Γ (with hyperperiod-length L) that is represented as K vectors of length L as follows: $[s_0^1, \dots, s_{L-1}^1], \dots, [s_0^K, \dots, s_{L-1}^K]$. On each vector, there are L intervals of length m of the form $X = [s_{t \bmod L}, s_{(t+1) \bmod L}, \dots, s_{(t+m-1) \bmod L}]$, $0 \leq t \leq L-1$ and hence, we have total $\lambda = KL$ number of intervals of length m . Let us consider

$$X_t^k(m) = [s_{t \bmod L}^k, s_{(t+1) \bmod L}^k, \dots, s_{(t+m-1) \bmod L}^k] \quad (11)$$

as the interval of size m starting from s_t^k on the k -th hyperperiod where $0 \leq t \leq L-1$ and $1 \leq k \leq K$. For all intervals $X_t^{(k)}(m)$, let us define the following variable:

$$C_t^k := \frac{1}{K} \left| \{k' : \delta(X_t^k(m), X_t^{k'}(m)) \leq \pi, 1 \leq k' \leq K\} \right|, \quad (12)$$

where $\delta(\cdot, \cdot)$ denotes the *dissimilarity* between two intervals of different hyperperiod, π is a given dissimilarity threshold and $|\cdot|$ represents the set cardinality. We use Hamming distance [35] to evaluate the dissimilarity between intervals – since this a relatively simple and widely used dissimilarity measure. For two vectors $U = [u_i]_{1 \leq i \leq m}$ and $V = [v_i]_{1 \leq i \leq m}$ of size m , Hamming distance is calculated as follows: $\delta(U, V) = \sum_{i=1}^m \mathbb{I}(u_i \neq v_i)$, where $\mathbb{I}(\cdot)$ is the indicator function that equals 1 if the condition (\cdot) is satisfied or 0 otherwise. Notice that, C_t^k represents the number of intervals of length m starting from s_t^k , $1 \leq k' \leq K$ with dissimilarity (in terms of Hamming distance) less than or equal to π from $X_t^k(m)$ and normalized by the number of observed hyperperiods (i.e., K).

Let us now define the variable η_t as an estimation of the entropy of variable $X_t^k(m)$, i.e., an estimation of the entropy of a vector that starts from slot t with length m as follows:

$$\eta_t = -\frac{1}{K} \sum_{k=1}^K \log_2 C_t^k. \quad (13)$$

Therefore for a given interval length $1 \leq m \leq L$ and dissimilarity threshold π , the randomness (entropy) of a schedule observed over K hyperperiods is given by the following equation:

$$\widehat{H}(\mathcal{S}^k, m, \pi, K) = \frac{1}{m} \sum_{t=0}^{L-1} \eta_t. \quad (14)$$

where η_t is given by Eq. (13).

Note that for $\pi = 0$, choosing $m = 1$ gives us $\widehat{H}(\mathcal{S}^k, m, \pi, K) = \widehat{H}(\mathcal{S}^k)$ and choosing $m = L$ outputs $\widehat{H}(\mathcal{S}^k, m, \pi, K) \rightarrow H(\mathcal{S}^k)$, as $K \rightarrow \infty$, where $\widehat{H}(\mathcal{S}^k)$ and $H(\mathcal{S}^k)$ are defined in Eqs. (10) and (9), respectively. Clearly, for a deterministic scheduler (e.g., vanilla EDF) the schedule entropy $\widehat{H}(\mathcal{S}^k, m, \pi, K)$ will be equal to *zero* (i.e., there is no randomness, as expected).

C. Evaluation of Schedule Entropy

In what follows we evaluate the REORDER protocol with synthetic workloads. This is to understand the degree of randomness introduced into the schedule and we used the proposed schedule entropy calculations from Section IV-B. The evaluation on a real embedded platform is presented in Section VI.

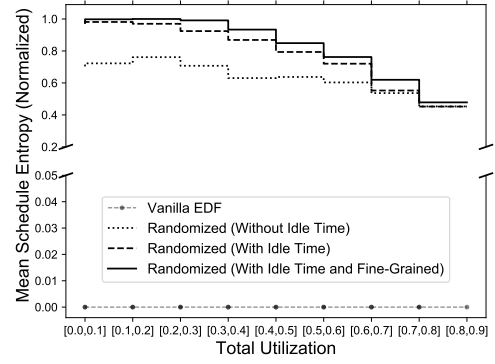


Fig. 3. The average entropy of the system with varying total utilization for different randomization schemes. The schedule shows maximum randomness (e.g., entropy) in the medium base-utilization (e.g., $[0.3, 0.7]$).

1) *Simulation Setup*: We used the parameters similar to that in earlier research [9], [12], [36], [37]. The tasksets were grouped by base-utilization (e.g., total sum of the task utilizations) from $[0.01 + 0.1 \cdot i, 0.1 + 0.1 \cdot i]$ where $i \in \mathbb{Z} \wedge 0 \leq i < 9$. Each base-utilization group contained 250 tasksets and each of which had $[3, 10]$ tasks. We only considered tasksets that were schedulable by EDF.

For a given base-utilization, the utilization U_i of individual tasks were generated from a uniform distribution using UUniFast [38] algorithm. The period of each task was greater than 10 with a divisor of 100. This allowed us to set a common hyperperiod (e.g., $L = 100$) for all the tasksets. We assumed that the deadlines are implicit, e.g., $D_i = T_i, \forall \tau_i$. The execution time C_i for each of the tasks in the taskset was computed using the generated period and utilization: $C_i = \lceil U_i T_i \rceil$. We set the interval window size $m = \lceil 0.35L \rceil$ and the dissimilarity threshold π was assumed to be $0.1L$ (see Appendix B). For each of the schedulable tasksets we observed the schedule for $K = 100$ hyperperiods.

2) *Results*: We now evaluate how much randomness (viz., unpredictability) the REORDER protocol incurs compared to vanilla EDF. In these experiments we focus on observing the *average behavior* of randomization schemes. In Fig. 3 we present the average schedule entropy of vanilla EDF (e.g., no randomization) along with different randomization schemes: (i) base randomization (only tasks are randomized), (ii) randomization with augmented tasksets (e.g., including idle time randomization) and (iii) fine-grained switching for augmented taskset (e.g., yielding tasks at random points).

The X-axis of Fig. 3 shows the total system utilization. The Y-axis represents mean schedule entropy (normalized to 1), e.g., $\widehat{H}_{mean}(\cdot) = \frac{1}{\hat{n}_s} \sum_{i=1}^{\hat{n}_s} \widehat{H}_i(\cdot)$, where \hat{n}_s represents the number of schedulable tasksets for a given base-utilization group and $\widehat{H}_i(\cdot)$ is the entropy of taskset i . Recall that for vanilla EDF entropy is zero since the same schedule repeats in every hyperperiod. As we can see from this figure, the randomization protocol significantly increases schedule entropy. The idle time randomization with fine-grained scheduling improves the entropy over base randomization. However for higher utilization the improvement is marginal. This is due the fact that for higher utilization, the system does not have enough slack (e.g., idle times) to randomize much – and hence all three schemes show similar results (in terms of schedule entropy). As the utilization increases (e.g., lesser slack), there are very

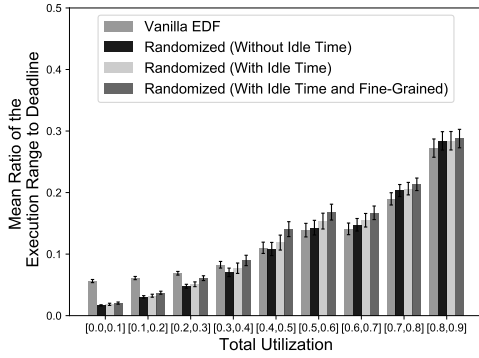


Fig. 4. The geometric mean of the execution range to the deadline ration. For REORDER the mean ratio is higher when utilization is greater than 0.4 – that implies the tasks appear in wider ranges and hence it is harder to infer the actual execution time.

few jobs for priority inversions because of higher load (less slack). As a result the entropy (*e.g.*, randomness) drops – albeit the schedule is still less predictable compared to the vanilla EDF (since the mean entropy is greater than zero).

Another way to observe the schedule randomness is to measure the ranges within which each task can appear. A wider range implies that is is harder to predict when a task executes. In this experiment we measured the first and the last time slots where a job of each task τ_i appears and used the difference between them as the range of execution for τ_i (denoted as w_i). In Fig. 4 we show the ratio of execution range to deadline (*e.g.*, $\frac{w_i}{D_i} \leq 1$) of the tasks. The X-axis of the figure shows total utilization and Y-axis represents the geometric mean of the task execution range to deadline ratios in each taskset.

In low utilization tasks appear within narrow ranges because of the work-conserving nature. With increasing utilization the ranges become wider. This is because the worst-case response times of tasks (particularly, for lower priority tasks) increases due to the higher loads. For lower utilization, the system is dominated by slack times and hence randomizing tasks do not improve the execution range compared to vanilla EDF. This is because, some (low-priority) jobs finish earlier due to priority inversions and hence response time of those jobs is actually lower than the EDF scheme. As a result mean ratio for REORDER decreases. As the figure shows, for higher utilization (*e.g.*, utilization greater than 0.4) tasks appear in wider ranges (*e.g.*, higher mean ratio) when REORDER is enabled. This is due to the fact that priority inversions with idle time randomization increase task response times (especially for higher priority tasks). Besides, inverting the priority can also move lower priority jobs closer to their release times, thus widening the range w_i .

V. IMPLEMENTATION

We implemented REORDER in a real-time Linux kernel running on a realistic embedded platform to validate its usability and to evaluate its overhead. To this end we also measure the overheads comparing this to an existing vanilla EDF scheduler. In this section we provide platform information and a high level overview of the implementation. We have open-sourced our implementation and make it available on a public repository [39]. The platform information and configurations are summarized in Table I.

Table I
SUMMARY OF THE IMPLEMENTATION PLATFORM

Artifact	Parameters
Platform	ARM Cortex-A53 (Raspberry Pi 3)
System Configuration	1.2 GHz 64-bit processor, 1 GB RAM
Operating System	Debian Linux (Raspbian)
Kernel Version	Linux Kernel 4.9.48
Real-time Patch	PREEMPT_RT 4.9.47-rt37
Kernel Configuration (make defconfig)	CONFIG_SMP disabled CONFIG_PREEMPT_RT_FULL enabled
Boot Commands	maxcpus=1
Run-time Variables	sched_rt_runtime_us=-1 scaling_governor=performance

A. Platform and Operating System

We used a Raspberry Pi 3 (RPi3) Model B⁴ development board as the base platform for our implementation. The RPi3 is equipped with a 1.2 GHz 64-bit quad-core ARM Cortex-A53 CPU developed on top of Broadcom BCM2837 SoC (System-on-Chip). RPi3 runs on a vendor-supported open-source operating system, *Raspbian* (a variant of Debian Linux). We forked the Raspbian kernel and modified it (refer to the following sections) to implement the REORDER protocol. Since we focus on the single core EDF scheduler in this paper, the multi-core functionality of RPi3 was deactivated by disabling the CONFIG_SMP flag during the Linux kernel compilation phase. The boot command file was also set with maxcpus = 1 to further ensure that the requirement of single core usage was satisfied.

B. Real-time Environment

The mainline Linux kernel does not provide any hard real-time guarantees even with the custom scheduling policies (*e.g.*, SCHED_FIFO, SCHED_RR). However the *Real-Time Linux (RTL) Collaborative Project*⁵ maintains a kernel (based on the mainline Linux kernel) for real-time purposes. This patched kernel (known as the PREEMPT_RT) ensures real-time behavior by making the scheduler fully preemptable. In this paper, we applied the PREEMPT_RT patch (version 4.9.47-rt37.patch.xz) on top of vanilla Raspbian (kernel version 4.9.48) to enable the real-time functionality. To further enable the fully preemptive functionality from the PREEMPT_RT patch, the CONFIG_PREEMPT_RT_FULL flag was enabled during the kernel compilation phase. Furthermore, the system variable /proc/sys/kernel/sched_rt_runtime_us was set to -1 to disable the throttling of the real-time scheduler. This setting allowed the real-time tasks to use up the entire 100% CPU utilization if required⁶. Also, the active core's scaling_governor was set to “performance” to disable dynamic frequency scaling and fix its frequency during the experiments.

C. Vanilla EDF Scheduler

Since Linux kernel version 3.14, an EDF scheduler implementation (known as SCHED_DEADLINE) is available in the kernel [20]. Since our custom PREEMPT_RT patched kernel supports SCHED_DEADLINE, we used this as the baseline EDF

⁴<https://www.raspberrypi.org/products/raspberry-pi-3-model-b/>.

⁵<https://wiki.linuxfoundation.org/realtime>.

⁶This change in system variable settings was mainly configured for the purpose of experimenting with the ideas of REORDER only. For most real use-cases, users can keep this system variable untouched for more flexibility.

implementation and extended the scheduler to implement the REORDER protocol.

In Linux the system call `sched_setattr()` is invoked to configure the scheduling policy for a given process⁷. By design, `SCHED_DEADLINE` has the highest priority among all the supported scheduling policies (e.g., `SCHED_NORMAL`, `SCHED_FIFO` and `SCHED_RR`). It's also worth noting that the Linux kernel maintains a separate run queue for `SCHED_DEADLINE` (i.e., `struct dl_rq`). Therefore, it is possible to extend `SCHED_DEADLINE` while keeping other scheduling policies unmodified. Note that this vanilla EDF scheduler is also used as a base for comparison with the REORDER protocol. The experimental results are presented in Section VI.

D. Implementation of Schedule Randomization Protocol

1) *Task/Job-specific Variables*: The Linux kernel defines a structure, `struct sched_dl_entity`, dedicated to `SCHED_DEADLINE`, to store task and job-related variables (both run-time and static variables). They include typical EDF task parameters (e.g., period, deadline and WCET). To implement REORDER we added two additional variables, named `redf_wcib` and `redf_rib`, both `s64` (signed 64 bit integer) type variables, to store the worst-case inversion budget (WCIB) for the task and to track the run-time inversion budget (RIB) for the task's active job at any given moment, respectively. Each task's `redf_wcib` is initialized and updated when a new task is created. The job-specific run-time variable, `redf_rib`, is initialized to the precomputed `redf_wcib` every time when a new job arrives. During run-time, the inversion budget was updated (i.e., decreased by the elapsed time in the case of priority inversion) along with other `SCHED_DEADLINE` run-time variables in the function `update_curr_dl()`. It is used to determine whether the inversion budget was consumed and a random selection of a job was allowed at a scheduling point.

In our implementations we did not use any external libraries and only used the built-in kernel functions. The following listing shows a part of the existing variables as well as the newly added ones (the highlighted lines). Other variables added for the REORDER protocol are shown in Appendix C.

```
struct sched_dl_entity {
/* task specific parameters */
    u64 dl_runtime;    // WCET
    u64 dl_deadline;   // relative deadline
    u64 dl_period;     // period
    s64 redf_wcib;     // worst-case inversion budget

/* task instance (job) specific parameters */
    s64 runtime;       // remaining runtime
    u64 deadline;      // absolute deadline
    s64 redf_rib;      // remaining inversion budget
    ....
/* Other variables are omitted for readability. */
};
```

2) *Task Selection Function*: The REORDER protocol was implemented as a function, named `pick_rad_next_dl_entity()`, that selects a task and sets the next scheduling point based on the REORDER algorithm. It replaces the original `SCHED_DEADLINE` function, `pick_next_dl_entity()` (i.e., one that picks the task

that has the next absolute deadline from the run queue, viz., the leftmost node in the scheduler's red-black tree). This function is indirectly called by the main scheduler function `__schedule()` when the next task for execution is needed.

3) *Randomization Function*: We used the built-in random number generator in the kernel. It supports the system call `get_random_bytes()` defined in `linux/random.h`. It is used by the function `pick_rad_next_dl_entity()` to select a random task and a random execution interval for the next scheduling point as explained in Algorithm 1.

4) *Schedule Timer*: A high-resolution timer (i.e., `struct hrtimer`) was used to trigger the additional scheduling points introduced by the REORDER protocol, as described in Algorithm 1 (Line 22 and 23). Since this timer is a scheduler-specific timer, it is stored in `dl_rq`, as `redf_pi_timer`. It is worth noting that `hrtimer` is also used by `SCHED_DEADLINE` to enforce the task periods.

5) *Idle Time Scheduling*: As introduced in Section III-C, idle times are considered when the idle time scheduling scheme is deployed. In our Linux kernel implementation, we utilized the native idle task maintained under the `SCHED_IDLE` scheduler for this purpose. The REORDER protocol yields its scheduling opportunities (to other schedulers such as `SCHED_IDLE`) if τ_I , the idle task in the REORDER protocol, is selected and running. The subsequent scheduling point is enforced by the aforementioned schedule timer `redf_pi_timer`.

VI. EVALUATION

In this section, we evaluate REORDER using a prototype implemented on an embedded platform (i.e., RPi3) running the real-time Linux kernel. We mainly focus on overheads for computing and selecting a task at each scheduling point. Recall that our implementation is based on the vanilla EDF scheduler, `SCHED_DEADLINE`, on Linux. Therefore, we evaluate the overheads of the REORDER protocol by comparing them with `SCHED_DEADLINE`.

The key observations from our performance evaluation results are summarized below.

- REORDER works in practice on realistic embedded RTS and is able to meet the real-time guarantees.
- The randomization logic adds minimal scheduling overhead in Linux kernel (Fig. 5). This overhead is arguably very small in comparison with the task execution time (Fig. 6).

1) *Experimental Setup*: We use the RPi3 platform as introduced in Section V. The operating system is patched and configured to enable the real-time capability, as shown in Table I. As mentioned earlier, the vanilla EDF scheduler in Linux is tested as a baseline to understand the degree of the overhead. To keep the vanilla EDF unpolluted from our implementation, we used two separately compiled kernels during the experiments. In the vanilla EDF kernel, the scheduling functions remained untouched. Only the necessary code to benchmark the overhead were added. Note that the aforementioned configurations that enable the real-time capability were still applied on this kernel.

For these experiments on the real platform, 800 synthetically generated tasksets were tested. The goal of the experiments was to evaluate the performance on synthetic workload on a real platform. Each taskset was configured with the number of tasks from 1 to 10 (10 groups). The utilization was set to

⁷Since there is no distinction between processes and threads in the Linux kernel's scheduler, for the simplicity of the illustration, we use the term *process*, *thread* and *task* interchangeably in the following context.

the range 10% and 90% (8 utilization groups, 10 tasksets per group) when generating the tasksets. Each task's period was randomly selected from the range 10ms and 100ms. Taskset parameters were randomly generated using the taskset generator from the simulation (see Section IV-C1). As a result, the generated parameters (e.g., the task's period and WCET) were multiples of 1ms. In the experiments, the actual execution time performed by a task τ_i was limited to $\lfloor 0.8 \cdot C_i \rfloor$ (i.e., 80% of its WCET) to accommodate realistic task execution behaviors. Both vanilla EDF and the randomized EDF were tested with the same set of tasksets.

To profile the number of context switches and random selections, we directly recorded their occurrence in the scheduler. We did not use external profiling tools with performance counters (e.g., perf [40]) because we only focus on the context switches that occur in the SCHED_DEADLINE scheduler (for both the vanilla EDF and the randomized EDF). Using the profiling tool may include unnecessary context switch counts from other coexisting Linux schedulers. To measure the execution time of the scheduling functions, the function `getnstimeofday()`, defined in `linux/timekeeping.h`, was used. For the experiments, we let a taskset run for 5 seconds. The measurements and the scheduling trace were stored in the kernel log for further analysis.

2) *Results:* We first examine the execution time overhead in both vanilla EDF and randomized EDF scheduling functions. As mentioned in Section V-D2, the main algorithm for the REORDER protocol was implemented in the function `pick_rad_next_dl_entity()`. This replaces the vanilla EDF scheduling function `pick_next_dl_entity()` in SCHED_DEADLINE. As this was the main change between the two schedulers, our test here was focused on measuring the execution time of `pick_next_dl_entity()` (for vanilla EDF) and `pick_rad_next_dl_entity()` (for REORDER) rather than the higher level scheduler function. In Fig. 5 we show the results of this experiment.

From the figure, we can observe that the mean execution cost of `pick_next_dl_entity()` for the vanilla EDF remains about the same across different taskset groups. This result is expected because the vanilla EDF always selects the leftmost node from the Linux red-black tree (i.e., run queue), which is independent to the number of tasks in a taskset and has complexity $O(1)$. On the other hand, the mean execution cost of `pick_rad_next_dl_entity()` for the base randomization (without idle time randomization) is generally larger than the vanilla EDF mainly due to the `get_random_bytes()` calls (which takes an average 2531 ns to generate a 64-bit random number) for the random task selections. When there is only one job in the run queue at a scheduling point, the base randomization scheme directly selects the job and omits the `get_random_bytes()` call. As a result, having fewer tasks in a taskset results in less frequent `get_random_bytes()` calls, and hence has smaller mean scheduling overhead. These experiment results suggest that the mean overhead increases as the number of tasks in a taskset increases. In the case of the idle time scheduling, since the idle task is always considered in every scheduling point, the algorithm reaches the final step with a randomly selected task most of the time. This leads to the overhead roughly corresponding to one `get_random_bytes()` call. For the fine-grained switching with idle time randomization scheme, the overhead remains a high level since, in the worst case, two `get_random_bytes()`

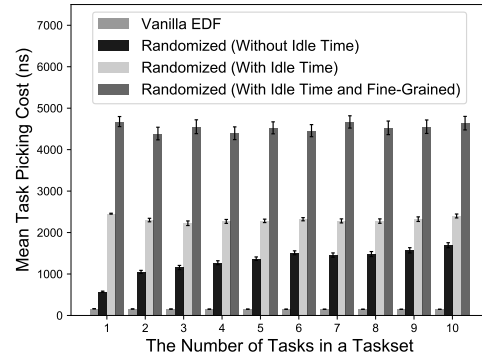


Fig. 5. The execution time cost (in nanoseconds) for the scheduling functions of the vanilla EDF and the randomized EDF. The vanilla EDF bar represents the mean execution times processed by the function `pick_next_dl_entity()` while the other three randomized EDF bars present the mean execution times for `pick_rad_next_dl_entity()` that carries out the randomization algorithm.

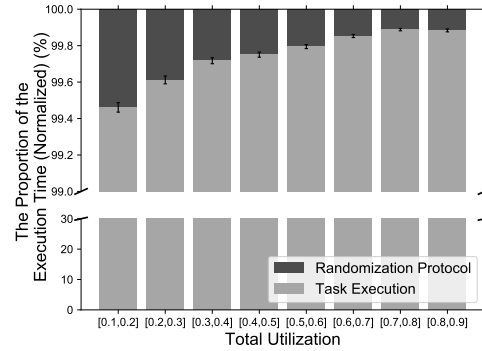


Fig. 6. The proportion of the cost of the REORDER protocol to the task execution times in the fine-grained switching with idle time randomization scheme. The randomization protocol overhead is provably inversely proportional to the taskset's total utilization. The upper part of the figure is scaled to 98% – 100% for better readability.

calls are present for each scheduling point: one for the random task selection and the other for the random scheduling points. This results in the scheduling overhead corresponding to the execution cost of two `get_random_bytes()` calls. As a result, the overhead contributed by the other part of the algorithm that has complexity $O(|\mathcal{R}_Q^t|)$ (as discussed in Appendix A) is negligible compared to the randomization function.

Next we examine the proportion of the scheduling overhead to the task's execution. We do this by comparing the cumulative time cost of the randomization protocol with the cumulative task execution times during the 5 second test duration for each taskset. Here, we consider the fine-grained switching with idle time randomization scheme as it has the largest overhead among all possible schemes. Figure 6 shows the mean proportion of the cost of the REORDER protocol to the task execution times with varying total utilization under such a scheme. The results indicate that the overhead of the REORDER protocol is inversely proportional to the taskset's total utilization. Since a taskset with higher utilization spends more of its time executing jobs, it dilutes the influence from the overhead. The utilization group [0.8, 0.9] has an average of 0.12% overhead while it is 0.54% for the [0.1, 0.2] utilization group. Considering there is typically an overestimation in the range 5% and 15% for WCET [41], we argue that the overhead of the REORDER protocol is negligible for most RTS.

VII. DISCUSSION

Although in this work we only emphasized on the fact that the proposed randomization mechanism can reduce the predictability of conventional dynamic priority scheduling, this idea improves the security posture of future RTS in a more fundamental way. For any scheduling policy, one can infer the amount of information *leaked* from the system. This information, for instance, will be useful for the engineers to analyze the potential *vulnerability* (associated with timing inference attacks) of the given system.

Consider a schedule S outputted from the randomization protocol (referred to as *ground-truth process*) and let S' be the attackers (potentially semi-correct) observation about the schedule (noted as *observation*). We can define the information leakage as the amount of uncertainty (of the adversary) as follows: the uncertainty about the ground-truth process minus the attackers uncertainty (about true schedule) after receiving the (fuzzy) observation (i.e., the amount of the reduction of uncertainty due to receiving the observation). One can then use *mutual information* [33, Ch. 2] (e.g., $\sup_{\tilde{u}} I(S; S')$ where \tilde{u} is the possible decoding strategies that an adversary can use and $I(S; S') = H(S) - H(S|S')$ is the mutual information) between the ground-truth and the observation as a measure of leakage. A high dependency between the ground-truth and the observation leads to a high information leakage. This implies that the adversary can have a good estimation of the ground-truth. The frameworks developed in this work aims to increase the randomness of the output of the scheduler and reduce the dependency between S and the S' . This is because, for the randomized scheduler, there are more true schedules that are consistent with a given observation. We highlight that defining the exact relationship between the produced randomness and the leakage of the system will require further study. We intend to explore this aspect in future work.

While the proposed randomization protocol hardens the success of timing inference attacks (and hence improves the security), it is *not* free from trade-offs. For instance, as we observe in Fig. 5 and 6, the randomization logic adds extra overheads to the scheduler. In this work we did not attempt to derive any analytic upper-bound on the number of context switches. Our future work will focus on designing a *tunable framework* where the system engineers can control parameters depending on application requirements (e.g., for a given taskset Γ , limit the number of context switches up to ε_{cs} with a trade-off in $\Delta\%$ reduced randomness) that provide best trade-off between system performance and security.

Note that it may be possible that some (heavily utilized) tasksets can *not* be randomized and in that case both EDF and REORDER output the same schedule. For instance, let us consider the taskset $\Gamma_{ex3} = \{\tau_1, \tau_2, \tau_3, \tau_4\}$ with the following parameters: $C_1 = 5, C_2 = 8, C_3 = 9, C_4 = 20$ and $T_1 = 5, T_2 = 8, T_3 = 9, T_4 = 20$ (with $T_i = D_i, 1 \leq i \leq 4$). The taskset is schedulable by EDF since $\sum_{1 \leq i \leq 4} \frac{C_i}{T_i} = 0.997 < 1$. However, in this case the budgets (e.g., WCIB) are always negative for all the tasks, e.g., $V_1 = -2, V_2 = -1, V_3 = -4, V_4 = -4$. Therefore, at each scheduling point *all* the low-priority jobs will be excluded from priority inversion and only the shortest deadline job will be selected. This will result in the same schedule as EDF with zero entropy and thus the system may be exposed to similar vulnerabilities as EDF.

VIII. RELATED WORK

The closest line of work is TaskShuffler [9] where we proposed to randomize task schedules for fixed-priority (e.g., RM) systems. However the methods developed there are not directly applicable for dynamic priority systems. Unlike fixed priority systems, obfuscating schedules for EDF scheduling is not straightforward due to run-time changes to task priorities. Besides, as we describe in Section IV-A, the calculation of schedule entropy in prior work does not capture the randomness correctly for all scenarios.

Unlike our scheduler-level solution, Zimmer *et al.* [42] propose the mechanisms to detect the execution of unauthorized instructions that leverages the information obtained by static timing analysis. An architectural approach that aims to create hardware/software mechanisms to protect against security vulnerabilities is studied by Yoon *et al.* [5]. Threats to covert timing channels for RTS has been addressed in prior research for fixed-priority systems [43]. A scheduler-level modification is proposed in literature [44] that alters thread blocks (that may leak information) to the idle thread – the aim is to avoid the exploitation of timing channels while achieving real-time guarantees. The authors also developed transformed locking protocols for covert channels in shared resources [45].

The issues regarding information leakage through storage timing channels using architectural resources (e.g., caches) shared between real-time tasks with different security levels is introduced in the literature [12], [13] and further generalized [46]. The authors proposed a modification to the fixed-priority scheduling algorithm and introduced a state cleanup mechanism to mitigate information leakage through shared resources. However, this leakage prevention comes at a cost of reduced schedulability. All the aforementioned work, however, is focused on fixed-priority systems. Besides such countermeasures may not be completely effective against timing inference attacks that focus on the deterministic scheduling behaviors. REORDER works to break this inherent predictability of real-time scheduling by introducing randomness.

Bao *et al.* [47] model the behavior of the attacker and introduce a scheduling algorithm. Unlike hard RTS, the authors consider a system with aperiodic tasks that have *soft* deadlines. The proposed polynomial complexity algorithm provide a trade-off between side-channel information leakage and the number of deadline misses for the real-time tasks. To the best of our knowledge REORDER is the first work that focuses on obfuscating schedule timing information for dynamic priority RTS with hard deadlines.

IX. CONCLUSION

Malicious attacks on systems with safety-critical real-time requirements could be catastrophic since the attackers can destabilize the system by inferring the critical task execution patterns. In this work we focus on a widely used optimal real-time scheduling policy and make progress towards developing a solution for timing side-channel attacks. By using the approaches developed in this work (along with our open-source Linux kernel implementation) engineers of the systems can now have enough flexibility, as part of their design, to secure such safety-critical systems. While our initial findings are promising, we believe this is only a start towards developing a unified secure real-time framework in general.

APPENDIX

A. Algorithm

Algorithm 1 formally presents the proposed schedule randomization protocol. This event-driven algorithm executes at the scheduler-level and takes the augmented taskset Γ' as an input. At each scheduling decision point t , a ready job is (randomly) selected for scheduling and the next scheduling decision point t' is determined.

Algorithm 1 Schedule Randomization Protocol

Input: Augmented task set $\Gamma' = \Gamma \cup \{\tau_I\}$ and current scheduling point t
Output: The randomized schedule S_t and the next scheduling point t'

```

1:  $\mathcal{R}_Q^t :=$  set of ready jobs
2: Add the highest priority job to the candidate list, i.e.,  $\mathcal{C}_L^t := \{\mathcal{R}_Q^{HP}\}$ 
3: /* Search candidate jobs if the highest priority job has non-zero inversion budget */
4: if  $v_{HP} > 0$  then
5:   for each  $\tau_j \in \mathcal{R}_Q^t$  do
6:     if  $d_j \leq m_{HP}^t$  then
7:        $\mathcal{R}_Q^t := \mathcal{R}_Q^t \cup \{\tau_j\}$  /* add  $\tau_j$  to candidate list */
8:     end if
9:   end for
10: end if
11: if  $\mathcal{C}_L^t = \{\mathcal{R}_Q^{HP}\}$  then
12:   /* schedule the highest priority (shortest deadline) job */
13:    $S_t := \mathcal{R}_Q^{HP}$ 
14:   Set next scheduling point  $t' :=$  when new job arrives or current job completes
15: else
16:   /* randomly select a job  $\tau_R$  from  $\mathcal{C}_L^t$  */
17:    $S_t := \tau_R$ 
18:   if  $\tau_R = \mathcal{R}_Q^{HP}$  then
19:     Set next scheduling point  $t' :=$  when new job arrives or current job completes
20:   else
21:     /* set the next random scheduling point  $t'$  as a function of current job completion or budget expiration time (unless a new job arrives before  $t'$ ) */
22:      $\Delta t := \text{rand}(1, \min(\widehat{C}_R^t, \widehat{v}))$ 
23:     Set next scheduling point  $t' := t + \Delta t$ 
24:   end if
25: end if
26: /* return the scheduled job and the next scheduling point */
27: return  $(S_t, t')$ 

```

In Lines 3-10, the algorithm first selects the set of candidate jobs \mathcal{C}_L^t using the procedure described in Section III-B (see Step 1). If the highest priority job \mathcal{R}_Q^{HP} has negative inversion budget (e.g., $v_{HP} \leq 0$), it will be scheduled for execution (Line 13). Otherwise it schedules a random job from the candidate list (Line 17). If the selected job is the highest priority job, the next scheduling point t' is set when the job completes or a new job of another task arrives (Line 14 and 19). If the selected job is not the highest priority one, the algorithm selects t' when the current inversion budget expires, unless the job completes or a new job arrives before t' (Line 23).

The algorithm iterates over the jobs in the current ready queue \mathcal{R}_Q^t once and makes a single draw from the candidate list $\mathcal{C}_L^t \subseteq \mathcal{R}_Q^t$. Assuming a single draw from a uniform distribution (Line 17 and 22) takes no more than $O(|\mathcal{R}_Q^t|)$, the complexity of each instance of the algorithm is $O(|\mathcal{R}_Q^t|)$.

B. Comparison With True and Approximate Entropy

Recall that obtaining the true entropy (e.g., $H(\cdot)$) is not feasible in practice since it has an asymptotic complexity. Therefore, we compare approximate entropy (e.g., $\widehat{H}(\cdot)$) with $H(\cdot)$ by measuring the correlation observed from small tasksets.

For this we generate the tasksets that have $[3, 5]$ tasks with $T_i \in \{2, 4, 5, 10, 20\}$ where the task utilizations and WCET are generated using the approach described in Section IV-C1. Each taskset has a common hyperperiod $L = 20$ (this allows us to evaluate enough schedules for a reasonable time). For each taskset we observe the schedule for $K = 1500$ hyperperiods and estimate the true entropy. Given a fixed taskset, generating more unique schedules (e.g., $K \rightarrow \infty$) leads to actual entropy $H(\cdot)$ since more tasks appear at each slot. For approximate entropy $\widehat{H}(\cdot)$ we set the interval length $m = \lceil 0.35L \rceil$ and the dissimilarity threshold $\pi = 0.1L$ by trial-and-error and measure the correlation.

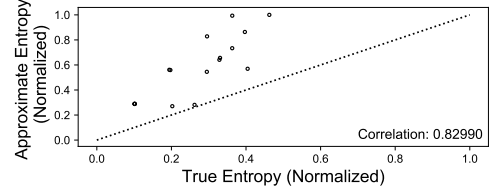


Fig. 7. The correlation between true and approximate entropy (the values are normalized to $[0, 1]$).

The true and approximate entropy do not depend on the length of the hyperperiod – instead, the approximation error (as can be seen from Figure 7) is due to the assumption of independence between intervals. While we observe that the correlation between true and approximate entropy is relatively high (e.g., ≈ 0.82) the approximated schedule entropy, $\widehat{H}(\cdot)$ should be used to compare the *relative randomness* of two schedules (that is also the focus of our evaluation).

C. REORDER Variables in Real-time Linux Implementation

The implementation of the REORDER protocol on the Linux kernel modifies four files:

- include/linux/sched.h (task/job-specific variables introduced in Section V-D1).
- kernel/sched/sched.h (scheduler-specific variables, as presented below).
- kernel/sched/core.c (scheduling functions that govern all schedulers in the kernel).
- kernel/sched/deadline.c (scheduling functions for SCHED_DEADLINE – the main REORDER algorithms were implemented here).

Besides the task-specific variables introduced in Section V-D1, there are scheduler-specific variables declared and used in our implementation, as shown in the listing below.

```

struct dl_rq {
    ...
    /* scheduler specific parameters */
    struct hrtimer redf_pi_timer; // schedule timer
    u64 redf_pi_timer_start_time; // timer start time
    bool redf_idle_time_acting; // idle time status
    enum redf_scheduling_mode redf_mode; // scheme
    ...
    /* other variables are omitted for readability. */
};

```

The variable `redf_mode` is used to determine the randomization scheme to be used in the scheduler. The enumeration for the scheme options are defined in the same source file (`kernel/sched/sched.h`) and shown in the following listing.

```
enum redf_scheduling_mode {
    REDF_NORMAL,           // task only randomization
    REDF_IDLE_TIME,        // with idle time scheduling
    REDF_FINE_GRAINED,     // with fine-grained switching
};
```

REFERENCES

- [1] J. Westling, "Future of the Internet of things in mission critical applications," 2016.
- [2] N. Falliere, L. O. Murchu, and E. Chien, "W32. Stuxnet dossier," *White paper, Symantec Corp., Security Response*, vol. 5, p. 6, 2011.
- [3] R. M. Lee, M. J. Assante, and T. Conway, "Analysis of the cyber attack on the ukrainian power grid," *SANS Industrial Control Systems*, 2016.
- [4] M.-K. Yoon, S. Mohan, J. Choi, J.-E. Kim, and L. Sha, "SecureCore: A multicore-based intrusion detection architecture for real-time embedded systems," in *IEEE RTAS*, 2013, pp. 21–32.
- [5] S. Mohan, S. Bak, E. Betti, H. Yun, L. Sha, and M. Caccamo, "S3A: Secure system simplex architecture for enhanced security and robustness of cyber-physical systems," in *ACM HiCoNS*, 2013, pp. 65–74.
- [6] M.-K. Yoon, S. Mohan, J. Choi, and L. Sha, "Memory heat map: anomaly detection in real-time embedded systems using memory behavior," in *ACM/EDAC/IEEE DAC*, 2015, pp. 1–6.
- [7] C.-Y. Chen, A. Ghassami, S. Nagy, M.-K. Yoon, S. Mohan, N. Kiyavash, R. B. Bobba, and R. Pellizzoni, "Schedule-based side-channel attack in fixed-priority real-time systems," Tech. Rep., 2015.
- [8] K. Jiang, L. Batina, P. Eles, and Z. Peng, "Robustness analysis of real-time scheduling against differential power analysis attacks," in *IEEE ISVLSI*, 2014, pp. 450–455.
- [9] M.-K. Yoon, S. Mohan, C.-Y. Chen, and L. Sha, "TaskShuffler: A schedule randomization protocol for obfuscation against timing inference attacks in real-time systems," in *IEEE RTAS*, 2016, pp. 1–12.
- [10] T. Xie and X. Qin, "Improving security for periodic tasks in embedded systems through scheduling," *ACM TECS*, vol. 6, no. 3, p. 20, 2007.
- [11] M. Lin, L. Xu, L. T. Yang, X. Qin, N. Zheng, Z. Wu, and M. Qiu, "Static security optimization for real-time systems," *IEEE Trans. on Indust. Info.*, vol. 5, no. 1, pp. 22–37, 2009.
- [12] S. Mohan, M.-K. Yoon, R. Pellizzoni, and R. B. Bobba, "Real-time systems security through scheduler constraints," in *IEEE ECRTS*, 2014, pp. 129–140.
- [13] R. Pellizzoni, N. Paryab, M.-K. Yoon, S. Bak, S. Mohan, and R. B. Bobba, "A generalized model for preventing information leakage in hard real-time systems," in *IEEE RTAS*, 2015, pp. 271–282.
- [14] M. M. Z. Zadeh, M. Salem, N. Kumar, G. Cutulenco, and S. Fischmeister, "SIPTA: Signal processing for trace-based anomaly detection," in *ACM EMSOFT*, 2014.
- [15] M. Hasan, S. Mohan, R. B. Bobba, and R. Pellizzoni, "Exploring opportunistic execution for integrating security into legacy hard real-time systems," in *IEEE RTSS*, 2016, pp. 123–134.
- [16] K. Krüger, M. Völpl, and G. Fohler, "Improving security for time-triggered real-time systems against timing inference based attacks by schedule obfuscation," in *ECRTS WiP*, 2017.
- [17] C. L. Liu and J. W. Layland, "Scheduling algorithms for multiprogramming in a hard-real-time environment," *JACM*, vol. 20, no. 1, pp. 46–61, 1973.
- [18] "Erika Enterprise," <http://erika.tuxfamily.org/drupal>.
- [19] "Real-time executive for multiprocessor systems (RTEMS)," <https://www.rtems.org>.
- [20] D. Faggioli, F. Checconi, M. Trimarchi, and C. Scordino, "An EDF scheduling class for the Linux kernel," in *Real-Time Linux Wkshp*, 2009.
- [21] A. K. Mok, "Fundamental design problems of distributed systems for the hard-real-time environment," Massachusetts Institute of Technology, Tech. Rep., 1983.
- [22] S. K. Baruah, A. K. Mok, and L. E. Rosier, "Preemptively scheduling hard-real-time sporadic tasks on one processor," in *IEEE RTSS*, 1990, pp. 182–190.
- [23] J. Y.-T. Leung and M. Merrill, "A note on preemptive scheduling of periodic, real-time tasks," *Inf. proc. letters*, vol. 11, no. 3, pp. 115–118, 1980.
- [24] D. Isovici, *Handling sporadic tasks in real-time systems: combined offline and online approach*. Mälardalen University, 2001.
- [25] J. Kelsey, B. Schneier, D. Wagner, and C. Hall, "Side channel cryptanalysis of product ciphers," in *Euro. Symp. on Res. in Comp. Sec.*, 1998, pp. 97–110.
- [26] D. Page, "Theoretical use of cache memory as a cryptanalytic side-channel," *IACR Crypt. ePrint Archive*, vol. 2002, p. 169, 2002.
- [27] D. A. Osvik, A. Shamir, and E. Tromer, "Cache attacks and countermeasures: the case of aes," in *Crypt. Track at the RSA Conf.*, 2006, pp. 1–20.
- [28] S. K. Baruah, "Resource sharing in EDF-scheduled systems: A closer look," in *IEEE RTSS*, 2006, pp. 379–387.
- [29] L. George, N. Rivierre, and M. Spuri, "Preemptive and non-preemptive real-time uniprocessor scheduling," INRIA, <https://hal.inria.fr/inria-00073732/file/RR-2966.pdf>, Tech. Rep., 1996, [Online].
- [30] M. Spuri, "Analysis of deadline scheduled real-time systems," INRIA, <https://hal.inria.fr/inria-00073920/file/RR-2772.pdf>, Tech. Rep., 1996, [Online].
- [31] J. P. Lehoczky, "Fixed priority scheduling of periodic task sets with arbitrary deadlines," in *IEEE RTSS*, 1990, pp. 201–209.
- [32] N. Audsley, A. Burns, M. Richardson, K. Tindell, and A. J. Wellings, "Applying new scheduling theory to static priority pre-emptive scheduling," *SE Journal*, vol. 8, no. 5, pp. 284–292, 1993.
- [33] T. M. Cover and J. A. Thomas, *Elements of information theory*, 2012.
- [34] S. M. Pincus, "Approximate entropy as a measure of system complexity," *Proc. of the Nat. Ac. of Sc.*, vol. 88, no. 6, pp. 2297–2301, 1991.
- [35] R. W. Hamming, "Error detecting and error correcting codes," *Bell Labs Tech. Journal*, vol. 29, no. 2, pp. 147–160, 1950.
- [36] A. Gujarati, F. Cerqueira, and B. B. Brandenburg, "Schedulability analysis of the Linux push and pull scheduler with arbitrary processor affinities," in *IEEE ECRTS*, 2013, pp. 69–79.
- [37] M. Bertogna and S. Baruah, "Limited preemption EDF scheduling of sporadic task systems," *IEEE Trans. on Ind. Info.*, vol. 6, no. 4, pp. 579–591, 2010.
- [38] E. Bini and G. C. Buttazzo, "Measuring the performance of schedulability tests," *RTS Journal*, vol. 30, no. 1–2, pp. 129–154, 2005.
- [39] "Implementation of Randomized EDF on Linux with RT Patch," <https://github.com/cchen140/RPi-RT-Linux>.
- [40] V. M. Weaver, "Linux perf_event features and overhead," in *FastPath*, vol. 13, 2013.
- [41] R. Wilhelm, J. Engblom, A. Ermedahl, N. Holsti, S. Thesing, D. Whalley, G. Bernat, C. Ferdinand, R. Heckmann, T. Mitra, F. Mueller, I. Puaut, P. Puschner, J. Staschulat, and P. Stenström, "The worst-case execution-time problem - overview of methods and survey of tools," *ACM Trans. Embed. Comput. Syst.*, vol. 7, no. 3, pp. 36:1–36:53, May 2008.
- [42] C. Zimmer, B. Bhat, F. Mueller, and S. Mohan, "Time-based intrusion detection in cyber-physical systems," in *ACM/IEEE ICCPS*, 2010, pp. 109–118.
- [43] J. Son and J. Alves-Foss, "Covert timing channel analysis of rate monotonic real-time scheduling algorithm in MLS systems," in *IEEE Inf. Ass. Wkshp*, 2006, pp. 361–368.
- [44] M. Völpl, C.-J. Hamann, and H. Härtig, "Avoiding timing channels in fixed-priority schedulers," in *ACM ASIACCS*, 2008, pp. 44–55.
- [45] M. Völpl, B. Engel, C. J. Hamann, and H. Härtig, "On confidentiality-preserving real-time locking protocols," in *IEEE RTAS*, 2013, pp. 153–162.
- [46] S. Mohan, M.-K. Yoon, R. Pellizzoni, and R. B. Bobba, "Integrating security constraints into fixed priority real-time schedulers," *RTS Journal*, vol. 52, no. 5, pp. 644–674, 2016.
- [47] C. Bao and A. Srivastava, "A secure algorithm for task scheduling against side-channel attacks," in *International Workshop on Trustworthy Embedded Devices*. ACM, 2014, pp. 3–12.